JOURNAL OF Materials CHEMISTRY

Disk-like liquid crystals of transition metal complexes

Part 21.‡—Critical molecular structure change from columnar to lamellar liquid crystal in bis(diphenylglyoximato)nickel(II)-based complexes

Kazuchika Ohta,*[a]† Ryuji Higashi,[ab] Mayumi Ikejima,[a] Iwao Yamamoto[a] and Nagao Kobayashi[b]

[a] *Department of Functional Polymer Science, Faculty of Textile Science & Technology, Shinshu University, Ueda, 386, Japan*

[b] *Department of Chemistry, Graduate School of Science, Tohoku University, Sendai, 980-77, Japan*

The critical molecular structure change from columnar to lamellar mesophases in bis(diphenylglyoximato)nickel(II)-based complexes has been investigated. When the number of the long chains surrounding the core complex part was reduced from eight to four, the mesophase changes its structure from columnar Col_{hd} to novel disk-like lamellar $D_{L.rec}(P2_12_1)$. When the length of the four chains at the *p*-positions was fixed and the remaining four chains at *m*-positions were gradually made shorter, each of the complexes shows a columnar Col_{ho} mesophase. Surprisingly, even when the substituents at *m*-positions are methoxy or methyl groups, a columnar Col_{ho} mesophase is still observed. When the substituents at *m*-positions were OH groups, another novel disk-like lamellar $D_{L.rec}(P2_11)$ mesophase is observed. Hence, it can be shown that the critical molecular structure change from the columnar to lamellar mesophase occurs between methoxy and hydroxy groups at the *m*-position. In both of the two novel $D_{L.rec}$ mesophases in the present study, the core complex parts are parallel to the layers and the long chains are normal to both the layers and the core complex planes. Such a unique mesophase structure has not been previously observed. The synthesis of these complexes and the temperature-dependent X-ray structural analyses of the unique mesophases are reported.

1 Introduction

Many types of organic transition metal complexes which are peripherally substituted by long chains affording columnar liquid crystalline properties have been reported. These columnar liquid crystals can self-organize to show much higher functionality than the unsubstituted non-mesogenic core complexes. For example, we reported that bis(diphenylglyoximato)-metal(II) (M = Ni, Pd, Pt) complexes[1] substituted with eight long alkoxy chains exhibit columnar mesophases and show other various properties, *e.g.*, thermochromism, solvatochromism and gelation. These properties originate not from the individual molecules but from their supramolecular structure. Furthermore, liquid crystalline compounds are also well known to dramatically change their supramolecular structure upon slightly changing the molecular structure. For example, long-chain-substituted bis(β-diketonato)copper(II) complexes reported by us[2] and long-chain-substituted perylene derivatives reported by Spieß and co-workers[3] dramatically change their liquid crystalline phase from calamitic to columnar upon slightly changing the number and length of the peripheral chains. Praefcke and co-workers also investigated the influence of the number and length of the peripheral chains on columnar mesomorphism.[4] The functionalities of materials depends on their supramolecular structures. Therefore, liquid crystalline compounds whose supramolecular structures can be controlled will play an important role in the development of functional materials.

As shown in Fig. 1, disk-like molecules containing more than six side-chains generally pile up one-dimensionally to give columnar mesophases. On the other hand, four-chain-substituted disk-like molecules tend to show disk-like lamellar (D_L) mesophases.[5–7] Although many columnar liquid crystalline compounds have been reported, a very few disk-like lamellar liquid crystals have been reported only for long chain-substituted bis(β-diketonato)copper(II) complexes,[5] long chain-substituted tetraphenylporphyrins[6] and tetrakis(alkyldithiolato)dinickel(II) complexes.[7] Two types of disk-like lamellar mesophases(D_{L1}, D_{L2}) have been found so far.[5] Here, we focused on our interest to prepare a new disk-like lamellar mesogen for bis(diphenylglyoximato)nickel(II)-based complexes. As described above, an eight-chain dodecyloxy group-substituted bis(diphenylglyoximato)nickel(II) complex [**1**: Ni(12,12) in Fig. 2] shows a hexagonal disordered columnar (Col_{hd}) mesophase. If the number of chains is reduced from eight to four, a new disk-like lamellar mesogen is expected to appear. Hence, initially we synthesized a four-chain dodecyloxy-substituted nickel complex [**5**: Ni(12) in Fig. 2]. As expected, Ni(12) shows a lamellar type of mesophase. Moreover, it unexpectedly has a novel disk-like lamellar rectangular ($D_{L.rec}$) mesophase, whose structure is quite different from those of the previous D_{L1} and D_{L2} mesophases. Nevertheless, we can state that when the number of the dodecyloxy chains surrounding the core Ni(DPG)$_2$ complex is reduced from eight to four, the mesophase changes its structure from columnar Col_{hd} to disk-like lamellar $D_{L.rec}$. We focused on our aim to investigate critical molecular structure changing from columnar to lamellar phase structure when the length of the four chains is fixed and the remaining four chains are gradually made shorter. Thus we synthesized complexes **2** and **3** (Fig. 2) which have four dodecyloxy chains at *p*-positions and four shorter chains at the *m*-positions. In the event, each of the complexes shows a columnar (Col_{ho}) mesophase. It is very surprising that even if the substituent at the *m*-position is a methoxy or methyl group, a columnar Col_{ho} mesophase is still obtained. When chains at the *m*-positions were finally removed, *i.e.* in complex **4** (Fig. 2) which has OH groups at the *m*-positions, a disk-like lamellar ($D_{L.rec}$) mesophase was eventually observed. Thus the critical molecular structure changing from columnar to lamellar mesophase occurs between $n = 0$ and 1 for alkoxy groups ($C_nH_{2n+1}O$) at *m*-positions. Furthermore, it is also seen that $D_{L.rec}$ in **4** has a lower symmetry than $D_{L.rec}$ in **5,** and that the two-dimensional rectangular lattice shrinks owing to a hydrogen-bonding network (HBN) in the layer compared to **5**. Surprisingly, in both

†E-mail: ko52517@giptc.shinshu-u.ac.jp

‡Part 20: ref. 1(f).

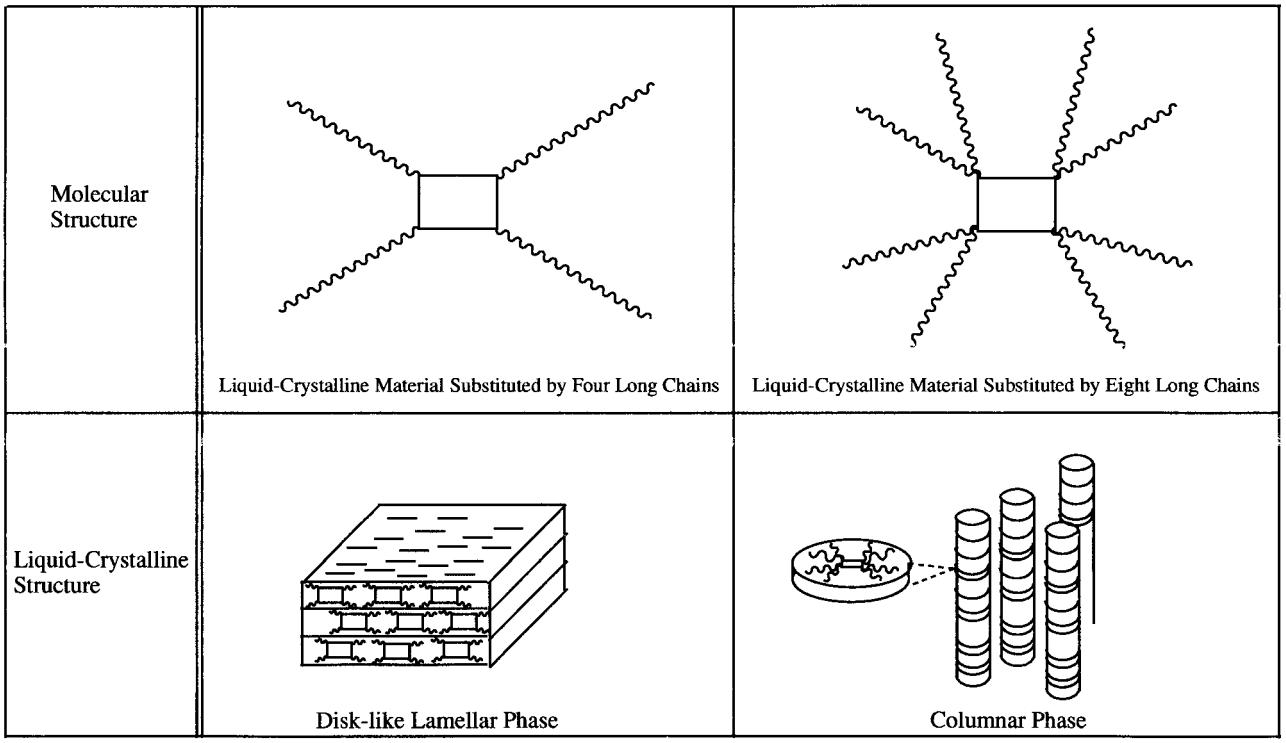

Fig. 1 Relationship between the molecular structures and the liquid-crystalline phases

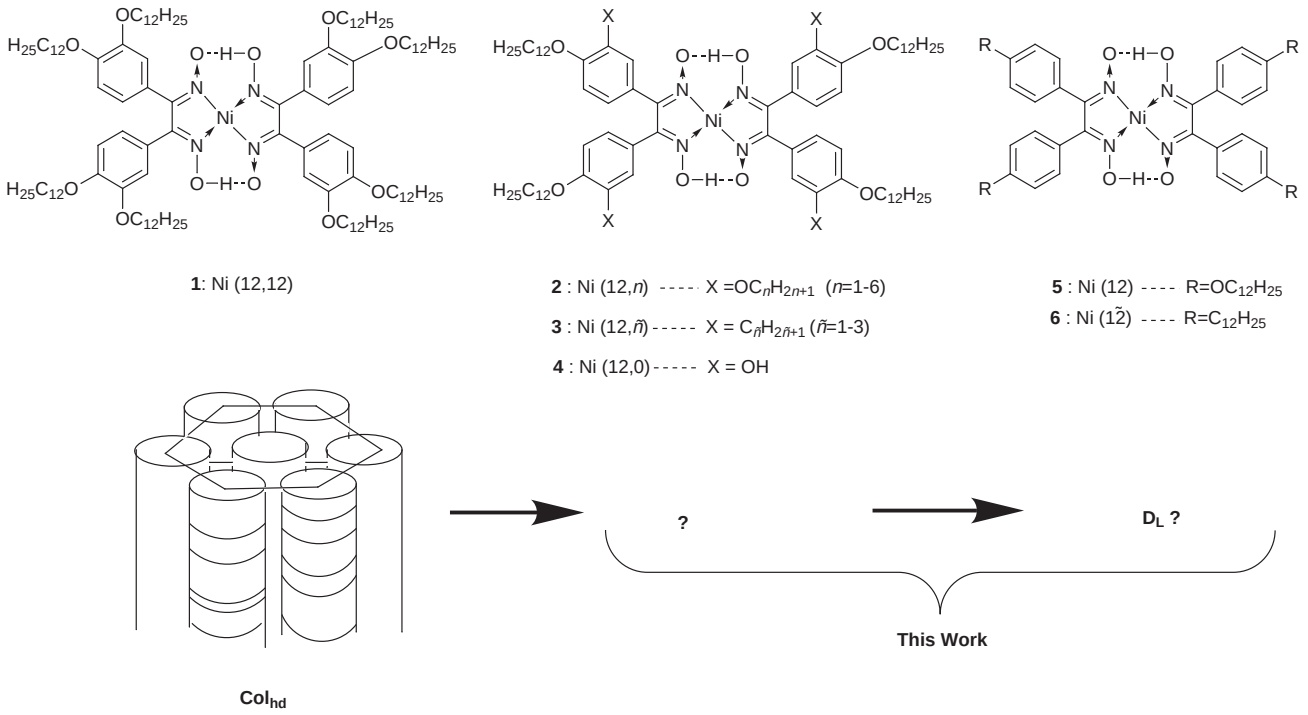

Fig. 2 Our strategy for pursuit of critical molecular structure changing from columnar to lamellar liquid crystal in the bis(diphenylglyoximato) nickel(II)-based complexes

of these two novel $D_{L.rec}$ mesophases, the core complex parts are parallel to the layers and the long chains are normal to both the layers and the core planes. Such a unique mesophase structure has not been previously observed. The long chains in conventional smectic, columnar and disk-like lamellar mesophases lie parallel to the core planes. Hence, one can change the long chains from parallel to normal to the core planes by changing the number (n) of carbon atoms at the m-position from $n=1$ to $n=0$, since the Ni(12,1) complex shows a conventional columnar mesophase whereas the Ni(12,0) complex exhibits a unique $D_{L.rec}$ mesophase.

We synthesized complex **6** containing four dodecyl chains only at the p-positions, in order to investigate the influence of oxygen atoms on the mesophase formation. Complex **6** showed only tetragonal columnar (Col_{tet}) mesophases attributable to dimerization which apparently leads to a disk unit composed of the dimer having eight long chains.

Thus, we found the critical molecular structure changing

from columnar to lamellar mesophase and two novel unique $D_{L.rec}$ mesophases.

2 Experimental

Fig. 3 illustrates the structural formulae of long-chain-substituted bis(diphenylglyoximato)nickel(II) complexes **1**–**6** of which **2**–**6** were synthesized in this work. The abbreviation of these complexes is composed of the central metal and the length of long chains in the two directions as M(*xy*); *x* and *y* being the numbers of carbon atoms along the *x* and *y* axis, respectively. Numbers *n* and *ñ* represent the numbers of carbon atoms in the alkoxy and alkyl chains, respectively.

Synthesis

Synthetic routes to complexes **2**–**6** are shown in Scheme 1. Detailed procedures of preparations of the precursors **7**, **13** and **14** have described in a previous paper.[8]

α-Diketone **8** which has only two dodecyloxy chains at *p*-position was prepared by reaction of the compound **7**[8] and dodecylbromide in the presence of potassium carbonate in *N*,*N*-dimethylacetoamide under a nitrogen atmosphere. The further *m*-alkylated α-diketone **9** was prepared by the same method for α-diketone **8**. 2-Alkyl dodecyloxybenzenes **11** were prepared by reaction of the commercially available compounds **10** and dodecyl bromide in the presence of potassium carbonate in *N*,*N*-dimethylacetoamide under a nitrogen atmosphere. Compounds **12** which possess two dodecyloxy groups and two short alkyl chains (methyl, ethyl or propyl), on the *p*- and *m*-positions, respectively were synthesized by Mohr's method.[9] The Ni(12,*n*):**2**, Ni(12,*ñ*):**3**, Ni(*n*,0):**4**, Ni(*n*):**5** and Ni(*ñ*):**6** complexes were synthesized by use of our previous method.[2] Detailed procedures are described below only for representative compounds. Table 1 lists the yields and elemental analysis data of all the complexes.

4,4′-Didodecyloxy-3,3′-dihydroxybenzil 8

3,3′,4,4′-Tetrahydroxybenzil **7**(2.1 g, 7.7 mmol), potassium carbonate (1.1 g, 8.0 mmol) and *n*-dodecyl bromide (4.35 g, 18.2 mmol) were added to 120 ml of *N*,*N*-dimethylacetoamide and the mixture stirred for 8 h at 70 °C under a nitrogen atmosphere. The reaction mixture was then extracted with diethyl ether and washed with water and the organic layer dried over anhydrous sodium sulfate. The solvents were removed under reduced pressure using a rotary evaporator and the crude product was purified by column chromatography using silica gel and chloroform and then by recrystallization from ethanol to give a white powder. Yield, 2.45 g (52%), m.p. 98 °C. ^{1}H NMR($CDCl_3$, TMS) δ 0.88(t, CH_3, 6H), 1.35–1.91(m, CH_2, 40H), 4.13(t, OCH_2, 4H), 5.74(s, OH, 2H), 6.82–7.59(m, aryl H, 6H). IR (Nujol, cm^{-1}) 3360(OH), 1670(C=O).

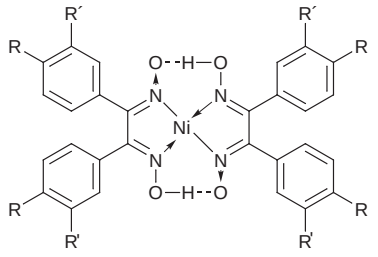

1	R = R′ = OC_nH_{2n+1}	: Ni(*n*,*n*) *n* = 4,8,12 [a]
2	R = $OC_{12}H_{25}$, R′ = OC_nH_{2n+1}	: Ni(12,*n*) *n* = 1-6
3	R = $OC_{12}H_{25}$, R′ = $C_{\tilde{n}}H_{2\tilde{n}+1}$	: Ni(12,*ñ*) *ñ* = 1-3
4	R = OC_nH_{2n+1}, R′ = OH	: Ni(*n*,0) *n* = 8,12,16
5	R = OC_nH_{2n+1}, R′ = H	: Ni(*n*) *n* = 10,12,14
6	R = $C_{\tilde{n}}H_{2\tilde{n}+1}$, R′ = H	: Ni(*ñ*) *ñ* = 12

This work

Fig. 3 Fomulae of the long chain-substituted bis(diphenylglyoximato)-nickel(II) complexes **1**–**6**. [a]Ref. 1(*a*)

4,4′-Didodecyloxy-3,3′-dipropyloxybenzil 9

4,4′-Didodecyloxy-3,3′-dihydroxybenzil, **8** (0.90 g, 1.5 mmol), potassium carbonate (0.43 g, 3.1 mmol) and *n*-propyl bromide (0.39 g, 3.2 mmol) were added to 70 ml of *N*,*N*-′dimethylacetoamide and the mixture stirred for 15 h at 90 °C under a nitrogen atmosphere. The reaction mixture was then extracted with chloroform and washed with water and the organic layer dried over anhydrous sodium sulfate. The solvent was removed under reduced pressure using a rotary evaporator and the crude product was purified by column chromatography using silica gel and chloroform and then recrystallized from ethanol to give a white powder. Yield 0.98 g (96%), m.p. 94.5 °C. ^{1}H NMR($CDCl_3$, TMS) δ 0.85–1.53(m, CH_3 and CH_2, 56H), 4.02(t, OCH_2, 8H), 6.65–8.09(m, aryl H, 6H). IR (Nujol, cm^{-1}) 1660(C=O).

2-Methyldodecyloxybenzene 11

2-Methyl phenol, **10** (2.00 g, 18.5 mmol), potassium carbonate (1.30 g, 9.41 mmol) and *n*-dodecyl bromide (4.66 g, 18.7 mmol) were added to 250 ml of *N*,*N*-dimethylacetoamide and the mixture stirred for 15 h at 100 °C under a nitrogen atmosphere. The reaction mixture was then extracted with chloroform and washed with water and the organic layer dried over anhydrous sodium sulfate. The solvents were removed under reduced pressure using a rotary evaporator and the crude product was purified by column chromatography using silica gel and chloroform to give a white syrup. Yield 4.31 g (80.8%). ^{1}H NMR($CDCl_3$, TMS) δ 0.68(t, CH_2CH_3, 3H), 1.08–1.80(m, CH_2, 20H), 2.01(s, aryl-CH_3, 3H), 3.58(t, OCH_2, 2H), 6.29–6.75(m, aryl, 4H).

4,4′-Didodecyloxy-3,3′-dimethylbenzil 12

To a mechanically stirred suspension of 2-methyldodecyloxybenzene **11** (2.00 g, 7.23 mmol) and aluminium chloride (1.06 g, 7.95 mmol) in 20 ml of carbon disulfide at 0 °C, was added a solution of oxalyl chloride (0.55 g, 4.3 mmol) in 10 ml of carbon disulfide over 1 h under a nitrogen atmosphere, and then the mixture was stirred for 5 h. After reaction the solvent was removed under reduced pressure using a rotary evaporator, the residue was extracted with dichloromethane and washed with water. The organic layer was dried over anhydrous sodium sulfate and the solvent removed under reduced pressure. The crude product was purified by column chromatography using silica gel and chloroform and then by recrystallization from ethanol to give a white powder. Yield 1.03 g (47.0%), m.p. 85.5 °C. ^{1}H NMR($CDCl_3$, TMS) 0.88(t, 6H, CH_3), 1.34–1.88(m, 40H, CH_2), 2.25(s, 6H, aryl-CH_3), 4.04(t, 4H, OCH_2), 6.80–7.83(m, 6H, aryl H). IR (KBr, cm^{-1}) 1655(C=O).

Bis[1,2-bis(4-*n*-dodecyloxy-3-butoxyphenyl)ethane dioximato]nickel(II); Ni(12,4): 2

Hydroxylamine hydrochloride (3.41 g, 49.1 mmol) and 85% potassium hydroxide (3.24 g, 49.1 mmol) were added to 100 ml of ethanol and the mixture vigorously stirred for *ca.* 1 h, and then filtered to remove the resulting precipitate of potassium chloride. 4,4′-Didodecyloxy-3,3′-dibutoxybenzil (0.59 g, 0.82 mmol) was added to the filtrate and the mixture refluxed with stirring under a nitrogen atmosphere for 15 h. Nickel(II) chloride hexahydrate (0.16 g, 0.67 mmol) dissolved in a small amount of ethane-1,2-diol was added to the hot reaction mixture and the resulting solution was then immediately neutralized with glacial acetic acid. After further refluxing for 4 h, the reaction mixture was cooled to room temperature. The reaction solvents were removed under reduced pressure

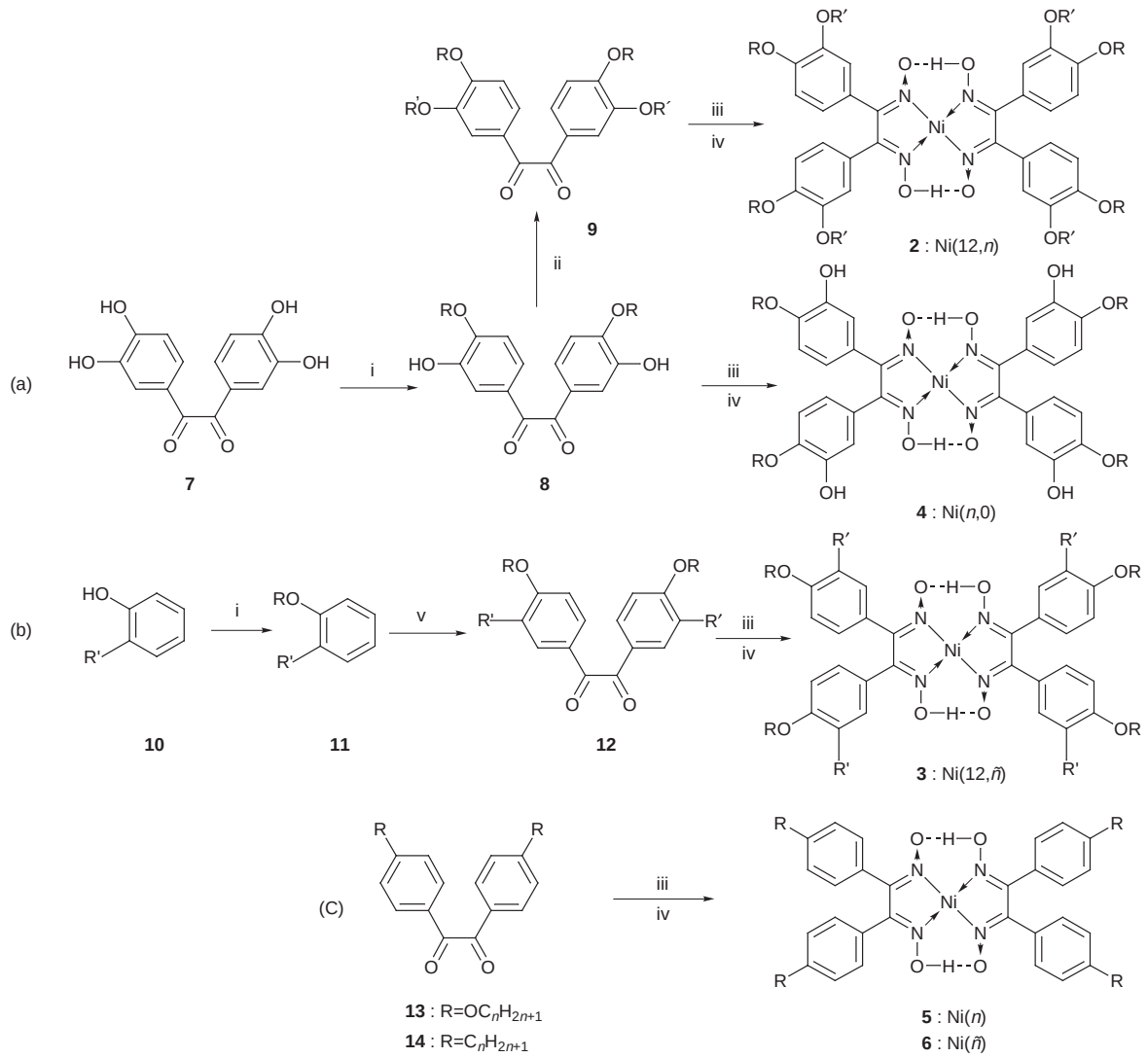

Scheme 1 Synthetic routes of the long chain-substituted bis(diphenylglyoximato)nickel(II) complexes **2**–**6**. *Reagents:* i, RBr, K_2CO_3/*N*,*N*-dimethylacetoamide; ii, R′Br, K_2CO_3/*N*,*N*-dimethylacetoamide; iii, $NH_2OH{\cdot}HCl$, KOH; iv, $NiCl_2{\cdot}6H_2O$/ethane-1,2-diol; v, $AlCl_3$, oxalyl chloride/CS_2.

Table 1 Yield and elemental analysis data for the long-chain-substituted bis(diphenylglyoximato)nickel(II) complexes, **2**–**6**

complex	$n(\tilde{n})$	yield (%)	molecular formula	molecular weight	elemental analysis (%) found (calc.) C	H	N
2: Ni(12,*n*)	1	18	$C_{80}H_{126}N_4O_{12}Ni$	1394.61	69.06(68.89)	9.17(9.11)	4.05(4.02)
	2	5	$C_{84}H_{134}N_4O_{12}Ni$	1450.17	69.34(69.54)	9.38(9.31)	3.72(3.86)
	3	43	$C_{88}H_{142}N_4O_{12}Ni$	1506.83	69.99(70.14)	9.60(9.50)	3.79(3.72)
	4	24	$C_{92}H_{150}N_4O_{12}Ni$	1562.93	70.74(70.69)	9.72(9.67)	3.59(3.58)
	5	25	$C_{96}H_{158}N_4O_{12}Ni$	1619.04	71.35(71.21)	10.03(9.84)	3.37(3.46)
	6	14	$C_{100}H_{166}N_4O_{12}Ni$	1675.15	71.75(71.69)	9.97(9.99)	3.05(3.34)
3: Ni(12,$\tilde{n}$)	$\tilde{1}$	5	$C_{80}H_{126}N_4O_8Ni$	1330.61	72.02(72.20)	9.59(9.54)	4.30(4.21)
	$\tilde{2}$	15	$C_{84}H_{134}N_4O_8Ni$	1386.72	72.68(72.74)	9.76(9.74)	3.98(4.04)
	$\tilde{3}$	11	$C_{88}H_{142}N_4O_8Ni$	1441.96	73.43(73.25)	10.06(9.92)	3.85(3.88)
4: Ni(*n*,0)	8	9	$C_{60}H_{86}N_4O_{12}Ni$	1114.07	64.97(64.69)	8.00(7.78)	4.74(5.03)
	12	19	$C_{76}H_{118}N_4O_{12}Ni$	1338.51	68.05(68.20)	8.89(8.89)	4.10(4.19)
	16	10	$C_{92}H_{150}N_4O_{12}Ni$	1562.94	70.65(70.70)	9.52(9.67)	3.52(3.58)
5: Ni(*n*)	10	24	$C_{68}H_{102}N_4O_8Ni$	1162.29	69.63(70.27)	9.03(8.85)	4.92(4.82)
	12	22	$C_{76}H_{118}N_4O_8Ni$	1274.51	71.48(71.62)	9.31(9.33)	4.38(4.40)
	14	16	$C_{84}H_{134}N_4O_8Ni$	1386.73	72.94(72.76)	9.71(9.74)	4.05(4.04)
6: Ni($\tilde{n}$)	$\tilde{12}$	17	$C_{76}H_{118}N_4O_4Ni$	1210.51	75.65(75.41)	9.52(9.83)	4.64(4.63)

using a rotary evaporator and the residue extracted with chloroform and washed with water. The organic layer was dried over anhydrous sodium sulfate, the solvent removed under reduced pressure and the crude product purified by column chromatography using silica gel and chloroform and then by reprecipitation by adding acetone to the chloroform solution to give red liquid crystals. Yield, 0.14 g (24%). ^{1}H NMR($CDCl_3$, TMS) δ 0.65–0.97(m, CH_3, 24H), 1.33–1.76(m, CH_2, 96H), 3.65(t, OCH_2, 8H), 3.92(t, OCH_2, 8H), 6.59–6.86(m, aryl H, 12H).

Bis[1,2-bis(4-*n*-dodecyloxy-3-methylphenyl)ethanedioximato]nickel(II); Ni(12,3): 3

Hydroxylamine hydrochloride (5.04 g, 72.6 mmol) and 85% potassium hydroxide (4.80 g, 72.6 mmol) were added to 125 ml of ethanol and the mixture vigorously stirred for *ca.* 1 h, and then filtered to remove the resulting precipitate of potassium chloride. To the filtrate 4,4′-didodecyloxy-3,3′-dimethylbenzil **12** (0.70 g, 1.15 mmol) was added and the mixture was refluxed with stirring under a nitrogen atmosphere for 15 h. Nickel(II) chloride hexahydrate (0.29 g, 1.22 mmol) dissolved in a small amount of ethane-1,2-diol was added to the hot reaction mixture and the solution was immediately neutralized with glacial acetic acid. After further refluxing for 4 h, the reaction mixture was cooled to room temperature and the reaction solvents were removed under reduced pressure using a rotary evaporator. The residue was extracted with chloroform and washed with water and the organic layer was dried over anhydrous sodium sulfate. The solvent was removed under reduced pressure and the crude product was purified by column chromatography using silica gel and chloroform and then by reprecipitation by adding methanol to the chloroform solution to give red liquid crystals. Yield, 0.040 g (5.0%). ^{1}H NMR ($CDCl_3$, TMS) δ 0.87(t, CH_2CH_3, 12H), 1.26–1.78(m, CH_2, 80H), 2.08(s, aryl- CH_3, 12H), 3.89(t, OCH_2, 8H), 6.52–7.09(m, aryl H, 12H).

Bis[1,2-bis(4-*n*-dodecyloxy-3-hydroxyphenyl)ethanedioximato]nickel(II); Ni(12,0): 4

Hydroxylamine hydrochloride (14.4 g, 207 mmol) and 85% potassium hydroxide (14.4 g, 218 mmol) were added to 100 ml of ethanol and the mixture stirred vigorously for *ca.* 1 h, and filtered to remove the resulting precipitate of potassium chloride. 4,4′-Didodecyloxy-3,3′-dihydroxybenzil **8** (2.00 g, 3.27 mmol) was added to the filtrate and the mixture was refluxed under an N_2 atmosphere with stirring for 15 h. Nickel(II) chloride hexahydrate (0.69 g, 2.90 mmol) dissolved in a small amount of ethane-1,2-diol was added to the hot reaction mixture and the solution was immediately neutralized with glacial acetic acid. After further refluxing for 4 h, the reaction mixture was cooled to room temperature and the reaction solvents removed under reduced pressure using a rotary evaporator. The residue was extracted with chloroform and washed with water and the organic layer was dried over anhydrous sodium sulfate. The solvent was removed under reduced pressure and the crude product purified by column chromatography using silica gel and *n*-hexane–ethyl acetate (1:1) and then by recrystallization from ethanol to give an orange powder. Yield, 0.41g (19%). ^{1}H NMR($CDCl_3$, TMS) δ 0.89(t, CH_3, 12H), 1.37–1.75(m, CH_2, 80H), 4.01(t, OCH_2, 8H), 5.55(s, OH, 4H), 6.72–6.87(m, aryl H, 12H).

Bis[1,2-bis(4-*n*-dodecyloxyphenyl)ethanedioximato]nickel(II); Ni(12): 5

Hydroxylamine hydrochloride (3.61 g, 51.9 mmol) and 85% potassium hydroxide (3.43 g, 51.9 mmol) were added to 86 ml of ethanol and the mixture stirred vigorously for *ca.* 1 h, and then filtered to remove the resulting precipitate of potassium chloride. 4,4′-Didodecyloxybenzil (0.50 g, 0.91 mmol) was added to the filtrate and the mixture was refluxed with stirring under an N_2 atmosphere for 17 h. Nickel(II) chloride hexahydrate (large excess; 2.04 g, 8.58 mmol) dissolved in a small amount of ethane-1,2-diol was added to the hot reaction mixture and the solution was immediately neutralized with glacial acetic acid. After further refluxing for 1 h, the reaction mixture was cooled to room temperature and the resulting precipitate collected by filtration and dissolved in chloroform. The organic layer was dried over anhydrous sodium sulfate and the solvent was removed under reduced pressure. The crude product was purified by column chromatography using silica gel and chloroform (R_f=0.80) and then by recrystallization from acetone–chloroform to give orange crystals. Yield, 0.13g (22%). UV–VIS ($CHCl_3$, 4×10^{-5} mol dm^{-3}) λ_{max}/nm= 381, 424, 461(sh). ^{1}H NMR($CDCl_3$, TMS) δ 0.88(t, CH_3, 12H), 1.26–1.76(m, CH_3, 80H), 3.90(t, CH_2, 8H), 6.68–7.11(m, aryl H, 16H).

Bis[1,2-bis(4-*n*-dodecylphenyl)ethanedioximato]nickel(II); Ni(12): 6

Hydroxylamine hydrochloride (3.83 g, 55.1 mmol) and 85% potassium hydroxide (3.83 g, 58.0 mmol) were added to 91 ml of ethanol and the mixture stirred vigorously for *ca.* 1 h, and then filtered to remove the resulting precipitate of potassium chloride. 4,4′-Didodecylbenzil (0.50 g, 0.86 mmol) was added to the filtrate and the mixture was refluxed with stirring under a nitrogen atmosphere for 17 h. Nickel(II) chloride hexahydrate (0.43 g, 1.8 mmol) which was dissolved in a small amount of ethane-1,2-diol was added to the hot reaction mixture which was immediately neutralized with glacial acetic acid. After further refluxing for 4 h, the reaction mixture was cooled to room temperature and the resulting precipitate collected by filtration and dissolved in chloroform. The organic layer was dried over anhydrous sodium sulfate and the solvent removed under reduced pressure. The crude product was purified by column chromatography using silica gel and chloroform (R_f= 0.91) and then by recrystallization from acetone to give orange crystals. Yield, 0.090 g (17%). ^{1}H NMR($CDCl_3$, TMS) δ 0.88(t, CH_2CH_3, 12H), 1.25–1.55(m, CH_2, 80H), 2.54(t, aryl- CH_2, 8H), 7.01–7.08(m, aryl H, 16H).

Measurements

The products were identified by elemental analyses using a Perkin Elmer 240B Elemental Analyzer. The phase transition behaviors of these compounds were observed by a polarizing microscope equipped with a heating plate controlled by a thermoregulator (Mettler FP80 and FP82), and measured with a Shimadzu DSC-50 differential scanning calorimeter. To establish the mesophases, powder X-ray patterns were measured with Cu-Kα radiation using a Rigaku Geigerflex instrument equipped with a hand-made heating plate controlled by a thermoregulator.

3 Results and Discussion

3.1 Mesomorphic properties of Ni(12,*n*):2 and Ni(12,*ñ*):3

We have already reported that the eight long-chain-substituted complexes Ni(*n*,*n*):**1** show a hexagonal disordered columnar (Col_{hd}) mesophase.[2a,b] In order to pursue the critical molecular structure changing from the columnar to the lamellar mesophase, we have synthesized the Ni(12,*n*):**2** complexes in which the alkoxy group at the *p*-positions is fixed as a dodecyloxy ($C_{12}H_{25}O$–) chain and the number of carbon atoms in the alkoxy group ($C_nH_{2n+1}O$) at the *m*-position is gradually reduced from n=6 to 1; *i.e.*, they gradually approach from eight long-chain-substituted complexes to four long-chain-substituted complexes. Then, we aimed to investigate the influence of the oxygen atom in the alkoxy group at the *m*-positions on the mesomorphic properties, and replaced alkoxy groups by alkyl groups ($C_{\tilde{n}}H_{2\tilde{n}+1}$: $\tilde{n}$=1, 2, 3) to obtain the Ni(12,*ñ*) complexes. The mesomorphism of these Ni(12,*n*) and Ni(12,*ñ*) complexes were studied.

The phase transition sequences, transition temperatures, enthalpy changes and lattice constants for mesophases of the Ni(12,*n*) and Ni(12,*ñ*) complexes are listed in Table 2. The Ni(12,*n*) (n=1–6) and Ni(12,3) complexes are dark red liquid crystals at room temperature. All of the Ni(12,*n*) and Ni(12,*ñ*) complexes show a considerable temperature region of a hexag-

Table 2 Phase transition sequences (T/°C) and enthalpy changes (ΔH/kJ mol^{-1} in parentheses) of the Ni(12,*n*) and Ni(12,$\tilde{n}$) complexes **2** and **3**[a]

complex	phase transitions
2: Ni(12,1)	$\mathrm{Col_{ho}}$ $\xrightarrow{297}$ IL (decomp.) $\{a=28.1$ Å, $h=3.33$ Å$\}$ at r.t. $\{a=28.1$ Å, $h=3.41$ Å$\}$ at 150 °C
Ni(12,2)	$\mathrm{Col_{ho}}$ $\xrightleftharpoons{245.9(13.6)}$ IL $\{a=28.8$ Å, $h=3.39$ Å$\}$ at r.t. $\{a=29.1$ Å, $h=3.47$ Å$\}$ at 150 °C
Ni(12,3)	$\mathrm{Col_{ho1}}$ $\xrightleftharpoons{105.6(4.43)}$ $\mathrm{Col_{ho2}}$ $\xrightleftharpoons{219.6(15.9)}$ IL $\{a=28.7$ Å, $h=3.38$ Å$\}$ at r.t. $\{a=29.1$ Å, $h=3.46$ Å$\}$ at 150 °C
Ni(12,4)	$\mathrm{Col_{ho}}$ $\xrightleftharpoons{206.5(25.0)}$ IL $\{a=29.2$ Å, $h=3.36$ Å$\}$ at r.t.
Ni(12,5)	$\mathrm{Col_{ho}}$ $\xrightleftharpoons{209.0(33.9)}$ IL $\{a=29.7$ Å, $h=3.38$ Å$\}$ at r.t.
Ni(12,6)	$\mathrm{Col_{ho}}$ $\xrightleftharpoons{187.5(35.3)}$ IL $\{a=28.0$ Å, $h=3.34$ Å$\}$ at r.t.
3: Ni(12,$\tilde{1}$)	K $\xrightleftharpoons{42.1(30.1)}$ $\mathrm{Col_{ho}}$ $\xrightleftharpoons{228.7(9.24)}$ IL $\{a=28.2$ Å, $h=3.35$ Å$\}$ at 170 °C
Ni(12,$\tilde{2}$)	K $\xrightleftharpoons{32.6(4.57)^b}$ $\mathrm{Col_{ho}}$ $\xrightleftharpoons{256.2(17.2)}$ IL $\{a=28.2$ Å, $h=3.35$ Å$\}$ at 170 °C
Ni(12,$\tilde{3}$)	$\mathrm{Col_{ho}}$ $\xrightleftharpoons{202.5(14.0)}$ IL $\{a=28.9$ Å, $h=3.50$ Å$\}$ at 170 °C

[a]Phase nomenclature: K = crystal, $\mathrm{Col_{ho}}$ = hexagonal ordered columnar mesophase and IL = isotropic liquid. [b]This small enthalpy change might be caused by a mixture of the K and $\mathrm{Col_{ho}}$ phases in the pristine sample.

onal ordered columnar ($\mathrm{Col_{ho}}$) mesophase. Interestingly, Ni(12,3) shows two types of $\mathrm{Col_{ho}}$ mesophases; $\mathrm{Col_{ho1}}$ (r.t.–105.6 °C) and $\mathrm{Col_{ho2}}$ (105.6–219.6 °C). However, the difference between them, as yet, is not clear. The lattice constants of the $\mathrm{Col_{ho2}}$ phase at 150 °C are almost the same as those of the $\mathrm{Col_{ho}}$ phase of Ni(12,1) and Ni(12,2) at 150 °C. It is most surprising that even the shortest methoxy group-substituted complex, Ni(12,1), shows a columnar $\mathrm{Col_{ho}}$ mesophase. This might be attributable to the oxygen atom in the methoxy group which would make the rectangular cores rotate readily so that they would appear as round disks. Hence, we then synthesized the Ni(12,$\tilde{n}$) complexes containing alkyl chains but no oxygen. The Ni(12,$\tilde{1}$) and Ni(12,$\tilde{2}$) complexes give a crystalline phase at room temperature and a $\mathrm{Col_{ho}}$ phase at higher temperatures. This means that free rotation is likely to be attributable to the influence of carbon rather than oxygen at the *m*-position. Table 3 lists X-ray diffraction data of the Ni(12,1) and Ni(12,$\tilde{1}$) complexes; each showed (100), (110), (200), [(210) only for Ni(12,1)] reflection lines in the low angle region corresponding to the two-dimensional hexagonal lattice, a sharp (001) reflection line in the medium angle region corresponding to the ordered stacking distance between the disks in the column, and a very broad halo corresponding to the melting of the chains.

Thus, we found that even if the substituents at the *m*-positions are methoxy or methyl groups, the carbon atom in the substituent makes them form a $\mathrm{Col_{ho}}$ mesophase. We also found no influence of oxygen atoms at *m*-positions on mesomorphism.

3.2 Mesomorphic properties of Ni(*n*,0):4 and Ni(*n*):5

We also synthesized the Ni(*n*,0):**4** and Ni(***n***):**5** complexes in which carbon atoms in the *m*-positions were absent and investigated their mesomorphism. Table 4 lists the phase transition sequences, transition temperatures, enthalpy changes and lattice constants for mesophases of the Ni(*n*,0), Ni(*n*) and Ni(12) complexes. As can be seen from this table, Ni(8,0) is not mesogenic but both Ni(12,0) and Ni(16,0) show a disk-like lamellar mesophase.[8] Moreover, each of the Ni(*n*) complexes shows a disk-like lamellar phase similar to Ni(12,0) and Ni(16,0). The structures of these disk-like lamellar mesophases have been established by temperature-dependent X-ray diffraction. X-Ray diffraction data of representative Ni(12,0) and Ni(12) complexes are listed in Table 5.

3.2.1 Mesophase structure of Ni(*n*):5. As shown in Table 5, the X-ray diffraction pattern of the mesophase of Ni(12) at 120 °C showed (001), (002) and (003) reflections in the low angle region corresponding to a lamellar structure, and (110),

Table 3 X-Ray diffraction data of the Ni(12,1) and Ni(12,$\tilde{1}$) complexes **2** and **3**

complex	mesophase (temperature)	lattice constants/Å	spacing/Å		Miller indices (hkl)
			d_{obs}	d_{calc}	
2: Ni(12,1)	$\mathrm{Col_{ho}}$ (r.t.)	$a=28.1$ $h=3.33$	24.3	24.3	(100)
			14.1	14.1	(110)
			12.5	12.2	(200)
			ca. 4.8	—	—[a]
			3.33	—	(001)
3: Ni(12,$\tilde{1}$)	$\mathrm{Col_{ho}}$ (170 °C)	$a=28.4$ $h=3.36$	24.7	24.6	(100)
			14.2	14.2	(110)
			12.3	12.3	(200)
			9.24	9.31	(210)
			ca. 4.8	—	—[a]
			3.36	—	(001)

[a]Melt of the alkoxy chains.

Table 4 Phase transition sequences (T/°C) and enthalpy changes (ΔH/kJ mol^{-1} in parentheses) of the Ni(n,0), Ni(n) and Ni($\tilde{n}$) complexes **4**, **5** and **6**[a]

complex	phase transitions
4: Ni(8,0)	$K_1 \underset{(16.6)}{\overset{103.0}{\rightleftharpoons}}$ K_2 $\underset{(32.2)}{\overset{176.2}{\rightleftharpoons}}$ IL
Ni(12,0)	$K^b \underset{(1.89)}{\overset{105.4}{\rightleftharpoons}}$ $D_{L.rec.}(P2_11)$ $\underset{(53.4)}{\overset{170.1}{\rightleftharpoons}}$ IL $\left\{\begin{array}{l}a=18.0\ \text{Å}\\ b=14.0\ \text{Å}\\ c=34.4\ \text{Å}\end{array}\right\}$ at 150 °C
Ni(16,0)	$K_1 \underset{(6.02)}{\overset{40.6}{\rightleftharpoons}}$ $K_2 \underset{(6.87)}{\overset{56\text{–}75(\text{broad})^c}{\rightleftharpoons}}$ $D_{L.rec.}(P2_11)$ $\underset{(56.3)}{\overset{164.5}{\rightleftharpoons}}$ IL $\left\{\begin{array}{l}a=18.0\ \text{Å}\\ b=14.0\ \text{Å}\\ c=42.2\ \text{Å}\end{array}\right\}$ at 150 °C
5: Ni(10)	$K_1 \underset{(39.7)}{\overset{69.8}{\rightleftharpoons}}$ $D_{L.rec.}(P2_12_1)$ $\underset{(40.0)}{\overset{159.8}{\rightleftharpoons}}$ IL $K_2 \overset{85.4\ (81.8)}{\nearrow}$ $\left\{\begin{array}{l}a=22.2\ \text{Å}\\ b=15.7\ \text{Å}\\ c=31.1\ \text{Å}\end{array}\right\}$ at 120 °C
Ni(12)	$K_1 \underset{(33.0)}{\overset{69.0}{\rightleftharpoons}}$ $D_{L.rec.}(P2_12_1)$ $\underset{(45.6)}{\overset{148.8}{\rightleftharpoons}}$ IL $K_2 \overset{87.3\ (140.8)}{\nearrow}$ $\left\{\begin{array}{l}a=22.2\ \text{Å}\\ b=15.3\ \text{Å}\\ c=34.5\ \text{Å}\end{array}\right\}$ at 120 °C
Ni(14)	$K_1 \underset{(4.60)}{\overset{27.5}{\rightleftharpoons}}$ $K_2 \underset{(1.17)}{\overset{49.2}{\rightleftharpoons}}$ $K_3 \underset{(49.4)}{\overset{77.0}{\rightleftharpoons}}$ $D_{L.rec}\ (P2_12_1)$ $\underset{(50.0)}{\overset{141.2}{\rightleftharpoons}}$ IL $\left\{\begin{array}{l}a=22.6\ \text{Å}\\ b=15.9\ \text{Å}\\ c=38.6\ \text{Å}\end{array}\right\}$ at 120 °C
6: Ni($\tilde{12}$)	$\rightarrow \text{Col}_{tet1} \overset{85.4}{\longrightarrow}$ IL $\left\{\begin{array}{l}a=24.9\ \text{Å}\\ a'=10.2\ \text{Å}\\ b'=7.01\ \text{Å}\end{array}\right\}$ at r.t. fast $K_1 \underset{(58.2)}{\overset{115.3}{\rightleftharpoons}} \text{Col}_X(\text{Col}_{tet2})$ $\overset{120.5(33.1)}{\rightleftharpoons}$ IL slow $K_2 \overset{121.2}{\rightleftharpoons}$ IL (very slow cooling) rapid cooling

[a]Phase nomenclature: K = crystal, $D_{L.rec.}$ = disk-like lamellar rectangular mesophase, Col_{tet} = tetragonal columnar mesophase, Col_X = unidentified columnar mesophase and IL = isotropic liquid. [b]Several unidentified transitions were observed before the melting. [c]This peak was very broad.

(200), (210), (220) and (400) reflections in the medium angle region corresponding to a two-dimensional rectangular lattice; a very broad halo due to the melting of the alkyl chains was also located in the medium angle region. These reflections were also observed for mesophases in the Ni(10) and Ni(14) complexes. Table 4 lists lattice constants for all the Ni(n) complexes. As revealed from the extinction rules for two-dimensional rectangular lattices[10] the present lattices have $P2_12_1(=P2_1/a)$ symmetry.

Lattice constant c values can be calculated from the (00l) reflections in the low angle region and correspond to the distance between neighbouring layers. The lattice constant c values of Ni(10), Ni(12) and Ni(14) are 31.1, 34.5 and 38.6 Å, respectively (Table 4). Furthermore, the a and b values are surprisingly the same as those of a single crystal of the non-substituted core complex, Ni(DPG)$_2$, (orthorhombic, space group $Iba2$, $Z=4$, $a=15.1936$, $b=22.3500$, $c=7.109$ Å), for which X-ray analysis was carried out by Konno *et al.*[11] Thus, the a and b values of the long-chain-substituted Ni(n) complexes are completely independent of the chain length and equal to the a and b values of the non-substituted core complex. This means that the long alkoxy chains are normal to both the core complex planes and the layers whereas the core complex moieties are parallel to the layers.

Table 5 X-Ray diffraction data of the Ni(12,0) and Ni(12) complexes **4** and **5**

complex	mesophase (temperature/°C)	lattice constants/Å	spacing/Å		Miller indices (*hkl*)
			$d_{obs.}$	$d_{calc.}$	
4: Ni(12,0)	$D_{L.rec.}(P2_11)$ (150)	$a=18.1$	34.7	34.4	(001)
		$b=14.0$	17.2	17.2	(002)
		$c=34.4$	14.0	14.0	(010)[b]
			11.5	11.5	(003)
			11.1	11.1	(110)
			9.04	9.04	(200)
			7.63	7.59	(210)
			6.94	6.98	(020)
			6.48	6.51	(120)
			ca. 4.5	—	—[a]
			4.48	4.51, 4.52	(130),(400)
5: Ni(12)	$D_{L.rec.}(P2_12_1)$ (120)	$a=22.0$	34.3	34.5	(001)
		$b=15.3$	17.3	17.3	(002)
		$c=34.5$	12.3	12.5	(110)
			11.6	11.5	(003)
			11.0	11.0	(200)
			9.08	8.92	(210)
			6.42	6.27	(220)
			5.51	5.49	(400)
			ca. 4.6	—	—[a]

[a]Melt of the alkoxy chains. [b]This assignment is not in accordance with the extinction rule of $P2_12_1(=P2_1/a)$ symmetry.

The number (Z) of molecules per unit cell can be calculated to be *ca.* 4 by using the measured a, b and c values whereas Z is generally 2 for conventional two-dimensional rectangular lattices with $P2_12_1$ symmetry. Furthermore, although the core complex moieties are parallel to the layers, the lattice constant c value is equal to twice the alkoxy chain length as mentioned above. From these facts it can be concluded that this mesophase in the Ni(n):**5** complexes should have a bilayer structure as does the non-substituted core complex.[11]

Evidence for this phase structure could in principle come from the electronic absorption spectra of a thin film of the mesophase. It is well known that molecules of the core $Ni(DPG)_2$ complex align one-dimensionally to form metal chains. The Ni—Ni intermetal distance in these one-dimensional chains sensitively determines the band-shift of the d_{z^2}–p_z electronic transition.[2d] However, this mesophase does not show such a d_{z^2}–p_z electronic transition band indicating that the Ni—Ni intermetal distance is too wide to lead to such a transition. This is compatible with the results of X-ray diffraction studies.

Fig. 4 illustrates the structural model of the unique mesophase of Ni(12). The top view shows the two-dimensional rectangular lattice with $P2_12_1$ symmetry in the layer. The side view illustrates the bilayer structure and the alkoxy chains normal to the layers. The complete three-dimensional view illustrates the mesophase structure, combining the top and side views. This mesophase has a quite novel structure completely different from any type of mesophases reported so far. We denote this phase 'disk-like lamellar rectangular ($P2_12_1$) mesophase' [abbreviated as $D_{L.rec}(P2_12_1)$], from its structural characteristics.

3.2.2 Mesophase structure of Ni(n,0):4. As listed in Table 5, the X-ray diffraction pattern of the mesophase of Ni(12,0) showed (001), (002) and (003) reflections in the low angle region corresponding to a lamellar structure, and (010), (110), (200), (210), (020), (120) and (130)/(400) reflections in the low to medium angle regions corresponding to a two-dimensional rectangular lattice. Almost the same reflections were also observed for the mesophase in the Ni(16,0) complex. The lattice constant c values for Ni(12,0) and Ni(16,0) are almost equal to twice the alkoxy chain length as is the case for the

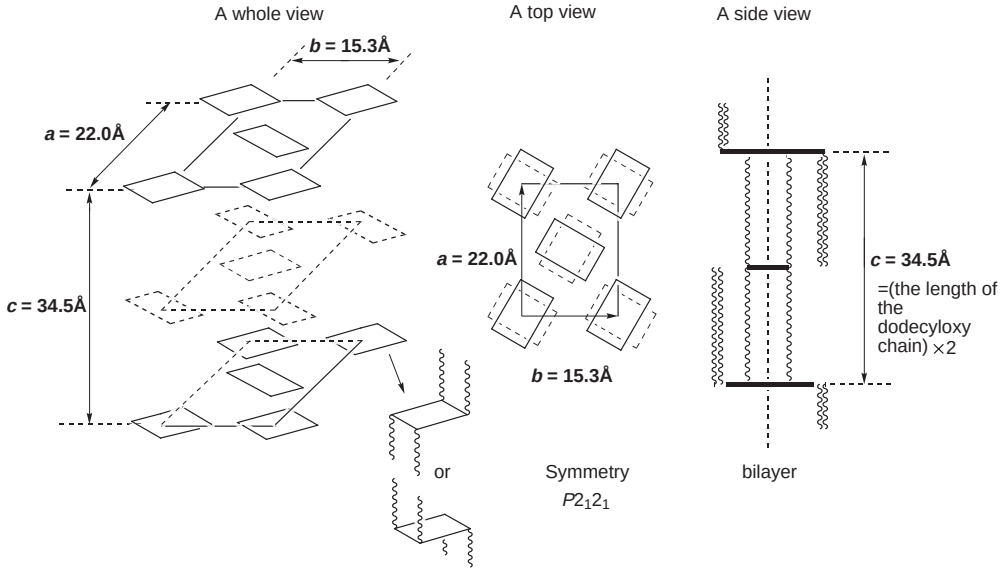

Fig. 4 Structural model of the novel lamellar mesophase of $D_{L.rec.}(P2_12_1)$ of the Ni(12) complex **5**

Ni(n) complexes. The lattice constant a and b values also do not change with change of alkoxy chain length (Table 4), as for the Ni(n) complexes. However, the a and b values are smaller than for the Ni(n) complexes (Table 4). This shrinkage can be attributed to formation of a hydrogen-bonding network (HBN) of the OH groups at the m-positions of the Ni(n,0) complexes in the layers, as illustrated in Fig. 5.

It was revealed from the temperature-dependent X-ray analysis (Table 5) that this mesophase has a unique structure that we have not encountered previously. The symmetry of this lattice was considered from the extinction rules for Miller indices. As described above, the symmetry of the two-dimensional rectangular lattice of the mesophase in the Ni(n) complexes is $P2_12_1(=P2_1/a)$. If the present mesophase in the Ni(n,0) complexes has the same $P2_12_1$ symmetry, the (010) reflection should disappear by the corresponding extinction rule of this symmetry [$h0$: $h=2n+1$, $0k$: $k=2n+1$] (Table 5); hence, the Ni(n,0) mesophases do not have $P2_12_1$ symmetry. Furthermore, if this lattice had $P2/a$ symmetry, one of the four symmetries for two-dimensional rectangular lattices reported so far,[10] two molecules must align per unit cell in the a-axis direction. If this was so, the lattice constant a should be much larger than that in $P2_12_1$ symmetry. By contrast, the a value of the present Ni(12,0) complex is smaller than that of the Ni(n) complexes. Moreover, from the extinction rule of $P2/a$ symmetry [$0k$: $k=2n+1$], the (010) reflection should disappear, hence, this mesophase does not have $P2/a$ symmetry. After similar considerations from the extinction rules of two two-dimensional rectangular lattices $C2/m$ and $P2m$ symmetries, they are also excluded. Therefore, this two-dimensional rectangular lattice seems to have a novel symmetry. We inferred that the molecular directions might be regularly controlled because the mesophase has a hydrogen-bonding network in the layers. On the other hand, since the lattice constant c values of Ni(12,0) and Ni(12) are the same, the long chains of Ni(12,0) should be normal to the core complex plane as for Ni(12). Accordingly, as illustrated in Fig. 6, two of the long alkoxy chains may extend upward and the other two chains downward,[12] so that the molecular direction can be assigned. In this figure, the direction from up to down is marked by an arrow and taking the resulting molecular direction into the symmetry considerations, the $P2_12_1$ symmetry is reduced to $P12_1$ or $P2_11$, as shown in Fig. 7. For $P12_1$ or $P2_11$ symmetry, a two-fold spiral axis exists in the b- and a-axis directions, respectively. In order to clearly distinguish these, these symmetries are denoted $P12_1$ and $P2_11$ following international crystallographic notation. As summarized in Table 6, the extinction rules are $0k$: $k=2n+1$ for $P12_1$ and $h0$: $h=2n+1$ for $P2_11$. Since this mesophase showed a (010) reflection, it can be concluded from these extinction rules that it has $P2_11$ symmetry. Therefore, we denote this phase 'disk-like lamellar rectangular ($P2_11$) mesophase' [abbreviated as $D_{L.rec}(P2_11)$] from its structural characteristics.

The control of the molecular orientations by the hydrogen-bonding network can be also proven by considerations from statistical thermodynamics. First from the measured enthalpy

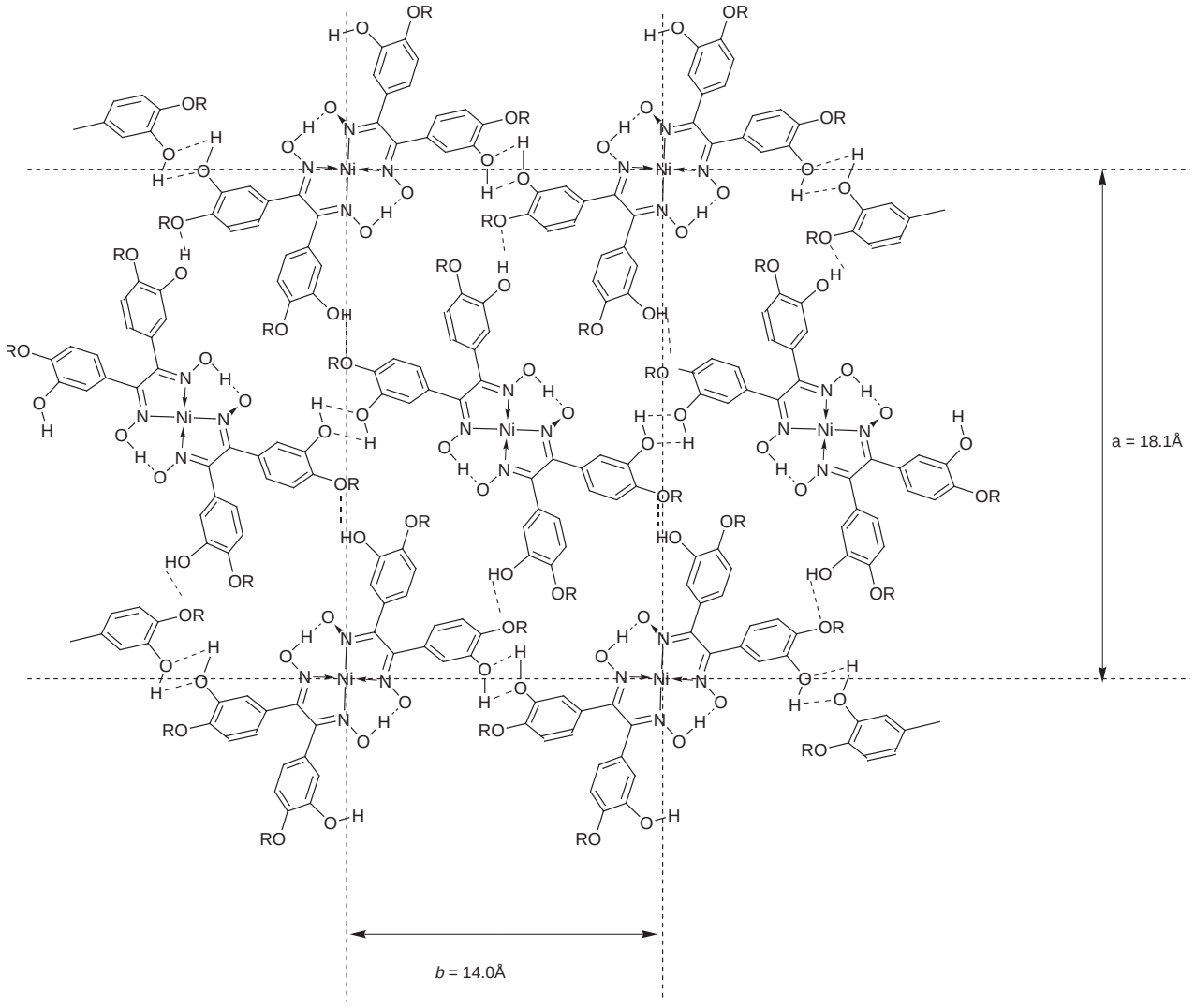

Fig. 5 Possible model of the lattice shrinking by the hydrogen-bonding network in the layer of the $D_{L.rec.}$ mesophase for the Ni(12,0) complex **4**

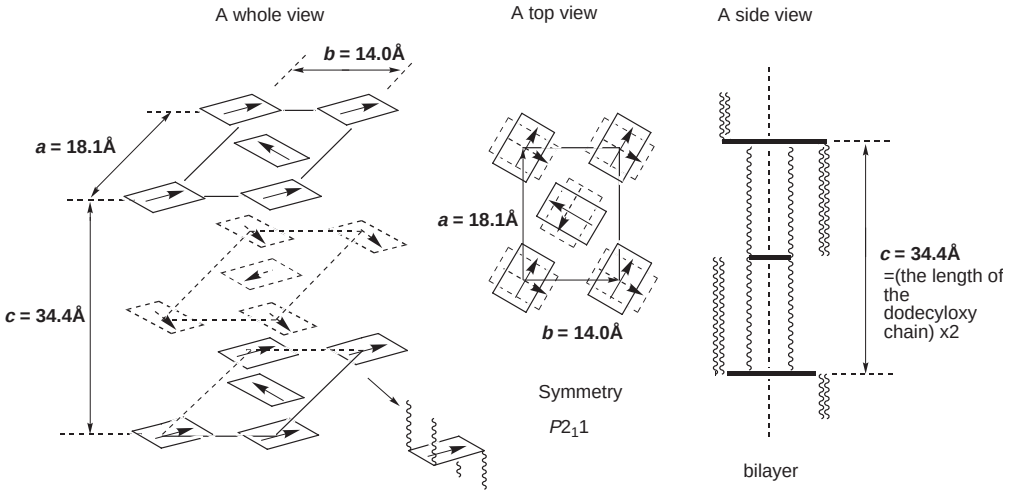

Fig. 6 Structural model of the novel lamellar mesophase of $D_{L.rec.}(P2_11)$ of the Ni(12,0) complex **4**. For this structure, the (010) reflection can be observed. See Table 5.

changes ΔH listed in Table 4, the experimental enthropy difference ΔS_{exp} between the entropy change $\Delta S_{Ni(12)}$ for the phase transition from $D_{L.rec}(P2_12_1)$ to isotropic liquid (IL) in Ni(12) and the entropy change $\Delta S_{Ni(12,0)}$ for the phase transition from $D_{L.rec}(P2_11)$ to IL in Ni(12.0) can be calculated.

$$\Delta S_{Ni(12,0)} = \Delta H/T = 53.4/(170.1+273.15) = 0.1205 \text{ kJ mol}^{-1}\text{ K}^{-1} = 120.5 \text{ J mol}^{-1}\text{ K}^{-1}$$

$$\Delta S_{Ni(12)} = \Delta H/T = 45.6/(148.8+273.15) = 0.1081 \text{ kJ mol}^{-1}\text{ K}^{-1} = 108.1 \text{ J mol}^{-1}\text{ K}^{-1}$$

$$\therefore \Delta S_{exp} = \Delta S_{Ni(12,0)} - \Delta S_{Ni(12)} = 120.5 - 108.1 = 12.4 \cong 12 \text{ J mol}^{-1}\text{ K}^{-1}$$

This experimental entropy difference ΔS_{exp} corresponds to the difference of molecular orientational order in the layers between $P2_11$ and $P2_12_1$ symmetries. Then, we theoretically calculate the entropy difference ΔS_{theor} by statistical thermodynamics. As illustrated in Fig. 8(A), the molecular directions in the mesophase having $P2_12_1$ symmetry are not fixed but random. In this case, a molecular direction has four possibilities; upper up, upper down, lower up, or lower down. Hence, the number of states W for Avogadro's number N of the molecules is 4^N.

$$\therefore W = 4^N$$

On the other hand, the molecular directions in the mesophase having $P2_11$ symmetry are fixed as shown in Fig. 8(B). Therefore, the entropy difference ΔS_{theor} between these mesophases can be calculated as;

$$\Delta S_{theor} = k \ln W = k \ln 4^N = kN \ln 4$$

where k is Boltzman's constant.

$$\therefore \Delta S_{theor} = 1.38 \times 10^{-23} \times 6.022 \times 10^{23} \times \ln 4 = 11.5 \cong 12 \text{ J mol}^{-1}\text{ K}^{-1}$$

Therefore,

$$\Delta S_{theor} = \Delta S_{exp}$$

This means that the control of the molecular orientations by the hydrogen-bonding network in the $D_{L.rec}(P2_11)$ mesophase can be also supported by statistical thermodynamics.

Fig. 6 illustrates the structural model of the unique

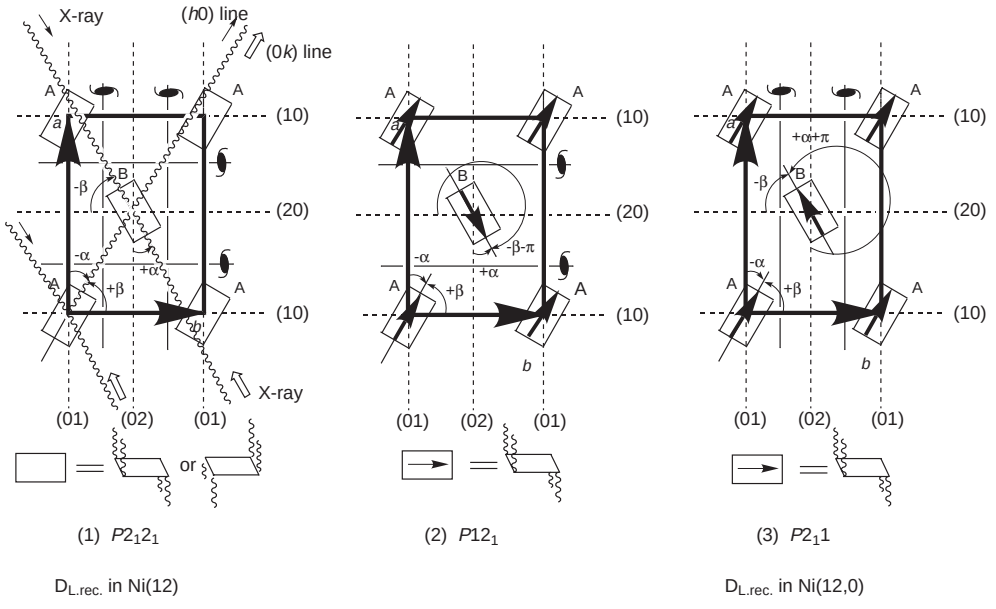

Fig. 7 Structures of the rectangular lattices having $P2_12_1$, $P12_1$ and $P2_11$ symmetries

Table 6 Extinction rules for the two-dimensional rectangular lattice shaving $P2_12_1$, $P12_1$ and $P2_11$ symmetries

symmetry	$P2_12_1$		$P12_1$		$P2_11$	
type of equivalent molecule	molecule A	molecule B	molecule A	molecule B	molecule A	molecule B
	$+\beta$	$-\beta$	$+\beta$	$-\beta-\pi$	$+\beta$	$-\beta$
tilt angle of the molecule from the (h0) line	$\therefore f_A=f_B=f$		$\therefore f_A\neq f_B$		$\therefore f_A=f_B=f$	
	$-\alpha$	$+\alpha$	$-\alpha$	$+\alpha$	$-\alpha$	$+\alpha+\pi$
tilt angle of the molecule from the (0k) line	$\therefore f_A=f_B=f$		$\therefore f_A=f_B=f$		$\therefore f_A\neq f_B$	
two-dimensional liquid crystalline structure factor: F	$F=f_A+f_B(-1)^{(h+k)}$		$F=f_A+f_B(-1)^{(h+k)}$		$F=f_A+f_B(-1)^{(h+k)}$	
extinction rule [(h,k) for $F=0$]	$h0{:}h=2n+1$				$h0{:}h=2n+1$	
	$0k{:}k=2n+1$		$0k{:}k=2n+1$			

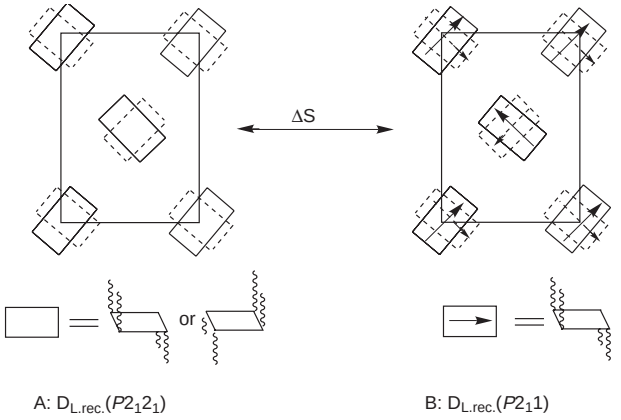

Fig. 8 Difference between the entropy changes of clearing for the $D_{L.rec.}(P2_12_1)$ and $D_{L.rec.}(P2_11)$ mesophases

mesophase $D_{L.rec}(P2_11)$ in Ni(12,0). Although this mesophase structure is basically the same as that of $D_{L.rec}(P2_12_1)$ in Ni(12), the molecular orientations are fixed by a hydrogen-bonding network and the two-dimensional rectangular lattice shrinks compared to that of $D_{L.rec}(P2_12_1)$ in Ni(12). Thus, this $D_{L.rec}(P2_11)$ mesophase has a novel structure completely different from any kind of mesophases reported to date.

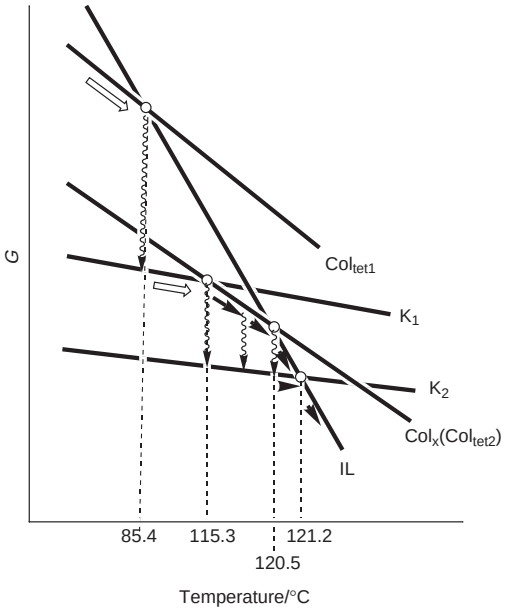

Fig. 9 Schematic free energy *vs.* temperature (G–T) diagram of the Ni(1̃2̃) complex **6**. ○: transition temperature; ⇒, →: heating; ⇝: relaxation.

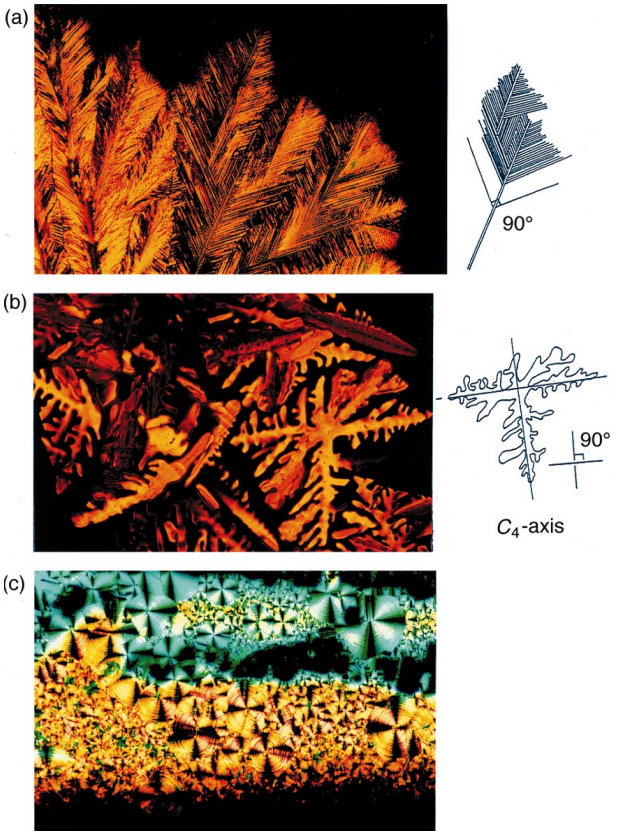

Fig. 10 Photomicrographs of the natural textures for the Col_{tet1} and Col_{tet2} mesophases of the Ni(1̃2̃) complex **6**. (a) The Col_{tet2} mesophase at 119.3 °C. The angle in this texture is 90°. (b) The Col_{tet2} mesophase at 120.6 °C. A four-fold axis of symmetry could be observed in this texture. (c) Fingerprint texture of the Col_{tet1} mesophase at r.t.

3.3 Mesomorphic properties of Ni(1̃2̃):6

The pristine state of the Ni(1̃2̃) complex, **6**, is a light orange needle-like crystalline phase (K_1) at r.t. When it was heated to 115.3 °C, the K_1 phase transformed into an unidentified columnar mesophase, Col_X, as indicated in Table 4. On further heating, the Col_X mesophase clears into an isotropic liquid phase, IL, at 120.5 °C. When the Col_X mesophase is slowly heated, it slowly relaxes into another plate-like crystal (K_2). The K_2 crystals melt into the IL at 121.2 °C. A red tetragonal columnar mesophase (Col_{tet1}) can be also obtained at r.t. when the IL at >122 °C is cooled rapidly. This Col_{tet1} mesophase melts into the IL at 85.4 °C in the second heating stage. This IL immediately crystallizes into the pristine state of the K_1 phase. When the IL at >122 °C is cooled very slowly, the K_2 crystalline phase can be obtained. On the other hand, when the IL is cooled at a moderate rate, the Col_X mesophase can be obtained. This complicated phase transition behavior can

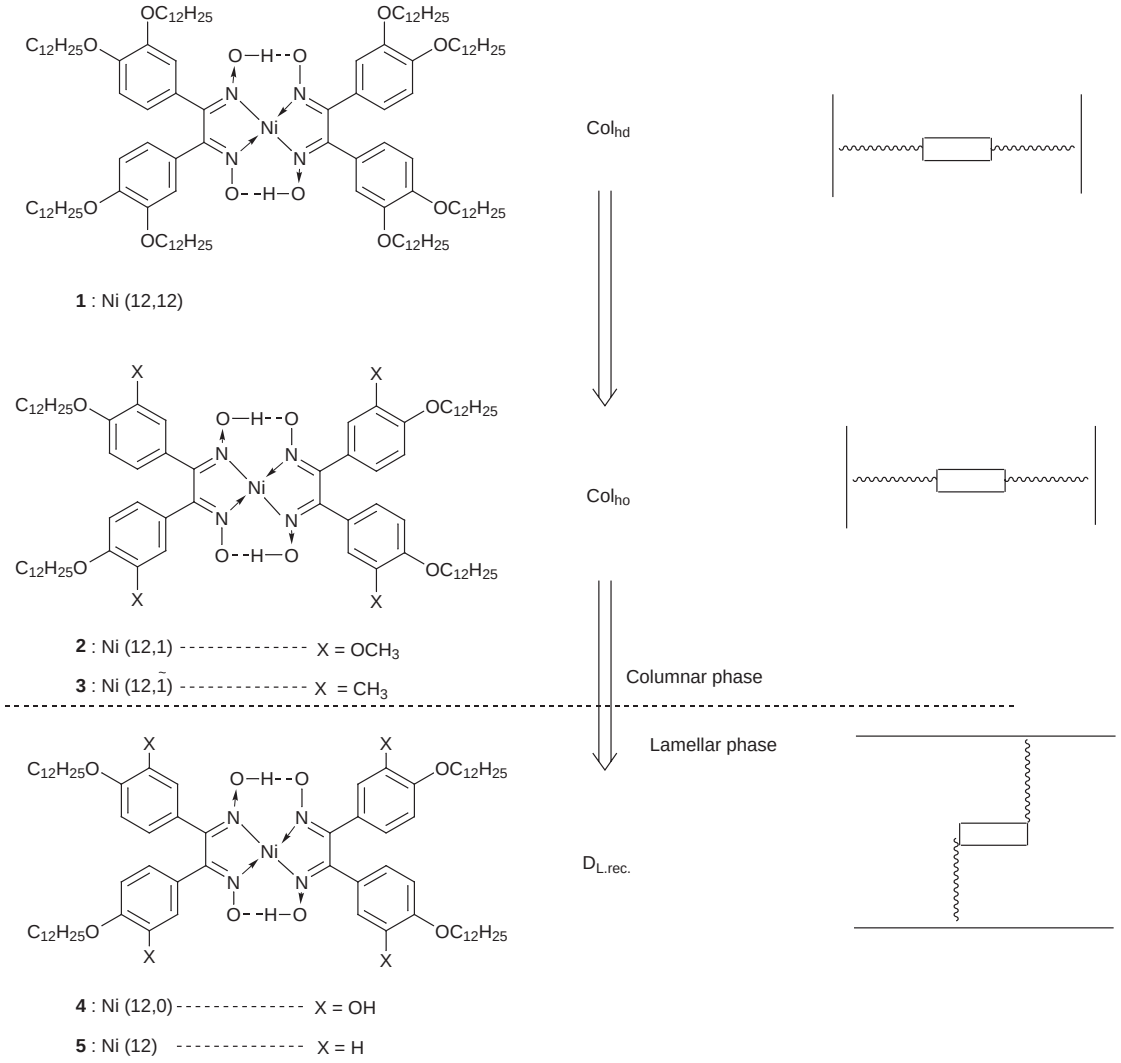

Fig. 11 The relationship between the molecular structure and the resulting mesophase structure for the bis(diphenylglyoximato)nickel(II)-based complexes. Critical change from the columnar mesophase to the lamellar mesophase occurs between **3** and **4**.

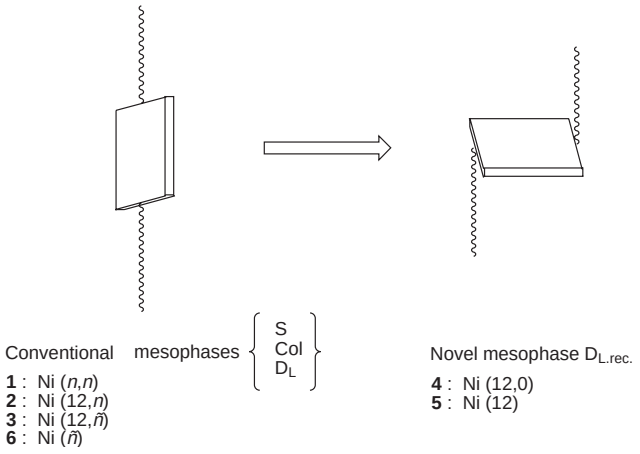

Fig. 12 Structural change from conventional mesophases (S, Col, D_L) to the novel mesophase($D_{L.rec}$)

be rationally explained by a schematic free energy *versus* temperature (*G*–*T*) diagram. For example, the heating process of the Col_{tet1} mesophase is illustrated in Fig. 9. When the Col_{tet1} mesophase is heated from r.t., it clears into the IL at 85.4 °C which corresponds to the intersection of the Col_{tet1} line and the IL line. The IL at 85.4 °C immediately relaxes and crystallizes into the metastable K_1 phase. On heating, this K_1 phase melts into the Col_X mesophase at 115.3 °C which corresponds to the intersection of the K_1 line and the Col_X line. The Col_X mesophase slowly relaxes into the K_2 phase. When the Col_X mesophase does not relax completely into the K_2 phase, the residue of the Col_X mesophase clears into the IL at 120.5 °C which corresponds to the intersection of the Col_X line and the IL line. This IL relaxes and crystallizes into the K_2 phase. The K_2 phase melts into the IL at 121.2 °C which corresponds to the intersection of the K_2 line and IL line. Thus, the complicated phase transition and relaxation behavior can be rationally explained by using the *G*–*T* diagram.

The natural texture of the Col_X mesophase could be obtained by moderate cooling as shown in Fig. 10. Fig. 10(a) shows a texture growing in four directions, the angle between each direction being 90°. Fig. 10(b) clearly shows a four-fold axis symmetry in this texture. This is very similar to the texture of the Col_{tet} mesophase of a tetrapyrazinoporphyrazine derivative.[13] Therefore, the present Col_X mesophase may also be identified as a Col_{tet} mesophase from these textures. However, it was impossible to carry out an X-ray diffraction study for the Col_X mesophase because of its narrow temperature region and the relaxation from the D_X mesophase into the K_2 phase. Considering these microscopic observations and the *G*–*T* diagram mentioned above, it can be deduced that the Col_X mesophase is another different Col_{tet} mesophase from the Col_{tet1} mesophase in the lower temperature region. Hence, we, tentatively denote the Col_X mesophase Col_{tet2}.

The natural texture of the Col_{tet1} mesophase obtained by rapidly cooling the IL to r.t. is a fingerprint-like texture, as is

shown in Fig. 10(c). The X-ray diffraction powder pattern of the Col_{tet1} mesophase gave twenty-three reflections corresponding to a two-dimensional tetragonal lattice having lattice constant $a = 24.9$ Å (Table 4). The pattern also gave three additional reflections corresponding to a rectangular lattice as the sub-lattice ($a' = 10.2$, $b' = 7.01$ Å). This sub-lattice may be ascribed to packing of the alkyl chains. The fact that so many reflections appear is attributed to the absence of any extinctions for a two-dimensional tetragonal symmetry. Since a diffuse band could be observed at $2\theta \approx 20°$, the packing of the long chains is somewhat disordered, although the presence of the sub-lattice suggests a degree of ordering of the packing of the long chains. As will be described elsewhere, the electronic spectra of a thin film of this Col_{tet1} mesophase exhibits a d–p transition band which implies that the central metals align in a one-dimensional manner. Columnar mesohphases are thus observed although the Ni(12) complex has only four long chains. This behavior may be attributable to dimerization by which a disk unit can apparently possess eight long chains.

4 Conclusion

As shown in Fig. 11, we continuously shortened the alkoxy chains at the *m*-position of the Ni(12,12):**1** complex exhibiting a columnar Col_{hd} mesophase to finally synthesize the methoxy-substituted Ni(12,1):**2** complex. It was found that this complex shows a columnar Col_{ho} mesophase. Furthermore, we synthesized the methyl-substituted Ni(12,$\tilde{1}$):**3** complex and found that it also shows a columnar Col_{ho} mesophase. It is very surprising that such short group-substituted Ni(12,1) and Ni(12,$\tilde{1}$) complexes also show a columnar mesophase. Finally, we removed the carbon atom at the *m*-position to synthesize the OH group *m*-substituted Ni(12,0):**4** and non-substituted Ni(12):**5** complexes.

These Ni(12,0) and Ni(12) complexes show novel lamellar ($D_{L.rec}$) mesophases. Therefore, we found that the critical change from columnar to lamellar mesophase occurs between $n = 0$ and 1 for alkoxy (OC_nH_{2n+1}) groups at *m*-positions.

Furthermore, we revealed the detailed mesophase structures of the $D_{L.rec}$ phases by temperature-dependent X-ray diffraction studies. The long chains in these $D_{L.rec}$ phases are normal to the core complex plane, whereas the long chains in conventional smectic(S), columnar(Col) and disk-like lamellar(D_L) mesophases are parallel to the core plane (Fig. 12). Such a unique mesophase structure is completely different from any kind of mesophase reported so far. It was also revealed from the extinction rules that the $D_{L.rec}$ mesophases of Ni(12,0) and Ni(12) have $P2_11$ and $P2_12_1$ symmetries, respectively. The molecular orientations in the $D_{L.rec}(P2_11)$ mesophase are fixed by a hydrogen-bonding network but not in the $D_{L.rec}(P2_12_1)$ mesophase. The two-dimensional rectangular lattice of the $D_{L.rec}(P2_11)$ mesophase shrinks as a consequence of the hydrogen-bonding network in the layer compared to that of the $D_{L.rec}(P2_12_1)$ mesophase.

Thus, we have observed two kinds of novel $D_{L.rec}$ mesophases and determined the critical molecular structure changing from lamellar to columnar liquid crystals.

References

1 M = Ni: (*a*) K. Ohta, H. Hasebe, M. Moriya, T. Fujimoto and I. Yamamoto, *Mol. Cryst. Liq. Cryst.*, 1991, **208**, 43; (*b*) K. Ohta, H. Hasebe, M. Moriya, T. Fujimoto and I. Yamamoto, *J. Mater. Chem.*, 1991, **1**, 831; M = Pd: (*c*) K. Ohta, M. Moriya, M. Ikejima, H. Hasebe, T. Fujimoto and I. Yamamoto, *Bull. Chem. Soc., Jpn.*, 1993, **66**, 3553; (*d*) K. Ohta, M. Moriya, M. Ikejima, H. Hasebe, T. Fujimoto and I. Yamamoto, *Bull. Chem. Soc., Jpn.*, 1993, **66**, 3559; M = Pt: (*e*) M. Ikejima, M. Moriya, H. Hasebe, T. Fujimoto, I. Yamamoto and K. Ohta, in *Chemistry of Functional Dyes*, ed. Z. Yoshida and Y. Shirota, Mita Press, Tokyo, 1993, vol. 2, p. 801; (*f*) K. Ohta, M. Ikejima, M. Moriya, H. Hasebe and I. Yamamoto, *J. Mater. Chem.*, 1998, **8**, preceding paper.

2 K. Ohta, H. Akimoto, T. Fujimoto and I. Yamamoto, *J. Mater. Chem.*, 1994, **4**, 61.

3 C. Göltner, D. Pressner, K. Müllen and H. W. Spieß, *Angew. Chem., Int. Ed. Engl.*, 1993, **32**, 1660.

4 B. Kohne and K. Praefcke, *Chem. Ztg.*, 1985, **109**, 121; B. Heinrich, K. Praefcke and D. Guillon, *J. Mater. Chem.*, 1997, **7**, 1363.

5 K. Ohta, H. Muroki, A. Takagi, K. Hatada, H. Ema, I. Yamamoto and K. Matsuzaki, *Mol. Cryst. Liq. Cryst.*, 1986, **140**, 131.

6 Y. Shimizu, M. Miya, A. Nagata, K. Ohta, A. Matsumura, I. Yamamoto and S. Kusabayashi, *Chem. Lett.*, 1991, 25.

7 K. Ohta, Y. Morizumi, H. Ema, T. Fujimoto and I. Yamamoto, *Mol. Cryst. Liq. Cryt.*, 1991, **208**, 55.

8 K. Ohta, H. Hasebe, H. Ema, M. Moriya, T. Fujimoto and I. Yamamoto, *Mol. Cryst. Liq. Cryst.*, 1991, **208**, 21.

9 B. Mohr, V. Enkelman and G. Wegner, *J. Org. Chem.*, 1994, **59**, 635.

10 T. Komatsu, K. Ohta, T. Watanabe, H. Ikemoto, T. Fujimoto and I. Yamamoto, *J. Mater. Chem.*, 1994, **4**, 537.

11 M. Konno, A. Kashima and I. Shirotani, *Z. Kristallogr.*, in the press.

12 I. Chambrier, M. J. Cook, M. Helliwell and A. K. Powell, *J. Chem. Soc., Chem. Commun.*, 1992, 444.

Paper 8/00897C; *Received* 2nd *February*, 1998